Journal of Molecular Catalysis A: Chemical 335 (2011) 242–247

Contents lists available at ScienceDirect

Journal of Molecular Catalysis A: Chemical

journal homepage: www.elsevier.com/locate/molcata

Efficient photoelectrocatalytic reduction of Cr(VI) using TiO_2 nanotube arrays as the photoanode and a large-area titanium mesh as the photocathode

Qing Wang, Jing Shang*, Tong Zhu, Fengwei Zhao

Department of Environmental Sciences, State Key Joint Laboratory of Environmental Simulation and Pollution Control, College of Environmental Sciences and Engineering, Peking University, Yiheyuan Road 5, Beijing 100871, People's Republic of China

ARTICLE INFO

Article history:
Received 22 October 2010
Received in revised form
27 November 2010
Accepted 29 November 2010
Available online 8 December 2010

Keywords:
Photoelectrocatalysis
Cr(VI)
TiO_2 nanotubes
Photocathode area
Reduction

ABSTRACT

We report the efficient photoelectrocatalytic (PEC) reduction of Cr(VI) using TiO_2 nanotubes (TNTs) as the photoanode and a large-area Ti mesh as the photocathode. Short-length TNTs (S-TNTs) show much greater PEC activity than either long-length TNTs (L-TNTs) or sol–gel-prepared TiO_2 film, due to the fact that the TNT structure is advantageous of trapping light energy over the thin-film structure and the S-TNTs enable the more efficient electron transfer into the substrate than L-TNTs. More importantly, increasing the surface area of the photocathode (Ti mesh) can greatly accelerate the PEC reduction of Cr(VI), presumably due to the increased number of the active reduction sites on the larger-surface Ti mesh. In the PEC reduction of Cr(VI), Cr(V) is identified as a reaction intermediate using the electroparamagnetic resonance technique, whereby the process for the Cr(VI) evolution is proposed. The S-TNTs have been confirmed to be stable over many repetitive cycles of use, indicating their suitability for wide-scale use.

1. Introduction

The general existence of Cr(VI) in the industrial wastewaters can cause harm to human health and the environment [1], due to its high toxicity and easy migration. Currently, the removal of Cr(VI) from wastewaters is through various physical means, such as the adsorption, ion exchange, and membrane filtration [2]. These methods cannot change the valence state of Cr(VI), but simply lead to the toxicity transfer. Cr(III) is another common oxidation state of chromium which is much less toxic and less mobile than Cr(VI). In fact, Cr(III) in low doses is an essential dietary mineral. It is reported that Cr(III) can be precipitated at basic pH and then removed as a solid waste [1,3]. Thus, it is of great value to reduce Cr(VI) to Cr(III) in the wastewater treatment.

Conventional chemical methods to reduce Cr(VI) to Cr(III) always result in chromium hydroxide sludge that is difficult to remove [2]. Since the late twentieth century, TiO_2 has emerged as a promising photocatalyst because of its high photocatalytic (PC) activity, non-toxicity, good stability, and low-cost fabrication [4,5]. Many researches have focused on the use of the TiO_2-based PC technique for the Cr(VI) reduction [6,7]. Under the acidic condition and in the presence of an organic compound that can act as a hole scavenger (e.g., dyes, citric acid, 4-chlorophenol), Cr(VI) can be effectively reduced to Cr(III), due to the efficient photogeneration of electrons in the conduction band (CB) of TiO_2 [8–10]. Most studies on the photoinduced reduction of Cr(VI) have been underlain by the aqueous suspensions of TiO_2 particles [3,11]. However, the practical application of TiO_2 powder is limited due to the difficulty of recycling particles. To circumvent this problem, TiO_2 film has been adopted for the PC reduction of Cr(VI) [7,12]. Unfortunately, because of the relatively small surface area of thin film, the resulting efficiency of the Cr(VI) PC reduction is substantially lower than that with a TiO_2 powder suspension. Yoon et al. demonstrated that with an initial concentration of Cr(VI) as low as 2 mg/L, the complete PC conversion of Cr(VI) to Cr(III) over TiO_2 nanotubes (TNTs) costed as long as 120 min [13].

To date, the mechanism of the PC reduction of Cr(VI) has not been determined. It is assumed that Cr(VI) is reduced sequentially to Cr(V), Cr(IV), and Cr(III) via one-electron steps [14,15]. Although both Cr(V) [15,16] and Cr(III) [7] have been detected during the reduction of Cr(VI), there has been no report on the quantitative variations of the Cr(VI), Cr(V), and Cr(III) concentrations over the reaction course.

Photoelectrocatalysis offers an advantage of restraining electron–hole recombination. The electric field can drive the photogenerated electrons migrating to the counter electrode, improving the separation of electron–hole pairs [17,18]. To date, the photoelectrocatalytic (PEC) reduction of Cr(VI) has rarely been considered. To our knowledge, there is only one study concerning the PEC reduction of Cr(VI) over TiO_2: using a sol–gel-prepared

* Corresponding author. Tel.: +86 10 62759716; fax: +86 10 62759716.
E-mail address: shangjing@pku.edu.cn (J. Shang).

1381-1169/$ – see front matter © 2010 Elsevier B.V. All rights reserved.
doi:10.1016/j.molcata.2010.11.040

TiO_2 thin film, 14.1 mg/L Cr(VI) was reduced completely at a scale of 60 min [19].

Recently, TNTs have been widely used in the PEC systems, because of their large surface area and good electron-transporting characteristics. For example, Liu et al. [20] studied the PEC oxidation of phenol using TNTs and found that shorter-length TNTs offered the better PEC efficiency. To date, the use of TNTs has been limited to the oxidation reactions; there is no reported study on the PEC reduction of Cr(VI) using TNTs as the photoanode. In general, the photocathode surface is the only occasion where the reduction reaction, $Cr_2O_7^{2-} + 14H^+ + 6e^- \rightarrow 2Cr^{3+} + 7H_2O$, takes place [19]. Thus, the efficiency of the PEC reduction of Cr(VI) is expected to be subject to the surface area of the photocathode.

Here, the PEC reductions of Cr(VI) over TNTs have been investigated. It is shown that the increase of the photocathode surface area greatly increased the efficiency of the PEC reduction of Cr(VI). The concentrations of Cr(VI), Cr(V), and Cr(III) over time were also monitored, giving rise to the proposal of describing the PEC reduction reaction of Cr(VI). Finally, the stability of the TNT photoanode was evaluated.

2. Experimental

2.1. Materials and reagents

Titanium sheets (99.7% in purity) and indium tin oxide (ITO)-coated glasses were commercially bought. Analytical-grade $K_2Cr_2O_7$, citric acid, NaCl, H_2SO_4, HF, and HNO_3 were obtained from Beijing Chemical Company (China). 2,2,6,6-Tetramethylpiperidine-1-oxyl (TEMPO, analytical grade) was purchased from Aldrich company. The water was purified in the lab using a Millipore filtration system with a resistivity of 18.25 MΩ cm. All the chemicals were used as received.

2.2. Preparation of TiO_2 electrodes

The patterned titanium sheets (76 mm × 26 mm) were rinsed with acetone, alcohol, and deionized water, consecutively, for 10 min in an ultrasonic bath. After drying in the air, the sheets were polished for 30 s in a mixture of HF, HNO_3, and water in 1:3:16 ratio, then rinsed in deionized water and dried in the air.

The anodization of one pre-cleaned Ti sheet was performed in a two-electrode cell connected to a DC power supply (HP-302D, HUAPU) with a platinum (Pt) foil as the counter electrode. Two kinds of different-length TNTs were prepared on the Ti sheets. Short-length TNTs (S-TNTs) were grown in the 0.5% (w/v) HF aqueous solution at pH = 5 and a bias of 20 V for 1 h, according to an established procedure [21]. Long-length TNTs (L-TNTs) were prepared in the 0.3% (w/v) NH_4F solution using 1% (v/v) water-dissolving ethylene glycol at a bias of 60 V for 17 h, as reported by Shanker et al. [22]. The obtained TNT anodes were rinsed with deionized water, then dried in the air, and finally annealed at 450 °C for 1 h.

The sol–gel-prepared TiO_2 film on ITO glass (denoted as TiO_2/ITO) was fabricated by a previously reported procedure [23]. The obtained TiO_2 films were confirmed anatase by the Raman spectra conducted on a JY HR800 spectrometer [23].

2.3. Characterization of TiO_2 electrodes

The morphologies and strucutres of the TiO_2 electrodes were studied using a field emission scanning electron microscope (FESEM, Nova Nano SEM 430) and an X-ray diffractor (XRD, DMAX-2400), respectively. The transient photocurrent in the TiO_2 photoanode was measured using a Keithley 2400 DC sourcemeter: the electrode was submerged in an 0.5 M NaCl solution with a Pt foil as its counterpart, and the interval between UV light on and off was 30 s.

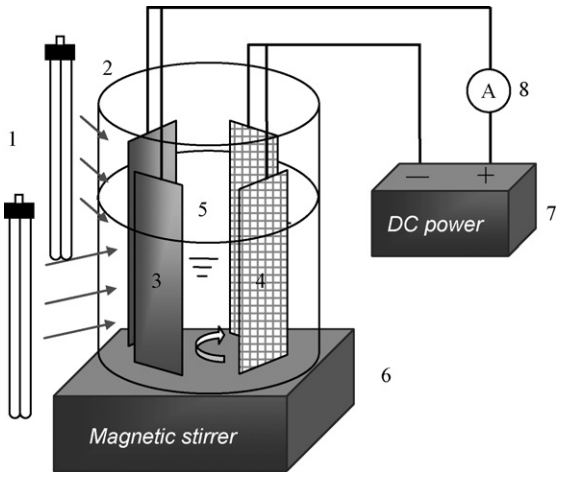

Scheme 1. Geometry of the reactor: (1) UV lamp; (2) quartz beaker; (3) TiO_2 photoanode; (4) Ti mesh photocathode; (5) $K_2Cr_2O_7$ solution; (6) magnetic stirrer; (7) DC power; (8) multimeter.

2.4. The reductions of Cr(VI)

The reductions of Cr(VI) were carried out in a quartz beaker which was 10 cm high and 7 cm wide in diameter. Two 8 W bacteria lamps with the primary wavelength of 254 nm were used as the UV light source, offering a light intensity of 3.1 mW/cm^2 at a distance of 5 cm to the light source. For each reduction of Cr(VI), a fresh solution (200 mL) containing 0.34 mM Cr(VI), 0.5 mM citric acid, 1 M NaCl, and pH = 2.5 was used. For the PEC reduction of Cr(VI), either Ti mesh with 0.25 mm openings or Pt foil was used as the photocathode. A bias of 1.5 V was appiled between the photoanode and photocathode by a DC power supply and the loop current was monitored by a digital multimeter. The geometry of the PEC setup is shown in Scheme 1.

The Cr(VI) concentration was monitored by measuring the absorbance of sampled solution at 349 nm by an UV–vis spectrophotometer (New Century, Model T6).

Changes in Cr(III) concentration were detected by the spectrophotometric method [24]. The sampled solution was added with 1–2 drops of EDTA solution which served as a chromogenic agent, followed by heating in water bath at 70 °C for 10 min to make the chromogenic reaction complete. Notice that the solution was ajusted to pH = 2.5 using sulphuric acid, as the chromogenic reaction proceeded in the acid condition. The reactive intermediate Cr(V) formed a complex with citrate in 1:1 ratio, which could be detected using the electroparamagnetic resonance instrument (EPR, a Bruker ESP 300 X-band spectrometer) [16]. TEMPO (g = 2.0051) was used as a reference to quantify the Cr(V).

3. Results and discussion

3.1. The morphologies and structures of the TiO_2 electrodes

Fig. 1 shows the FESEM images of three TiO_2 electrodes. The S-TNTs exhibited a length of ~248 nm with an outer diameter of ~55 nm and a wall thickness of ~8.1 nm, while the L-TNTs showed a length of 32.8 μm with an outer diameter of 148 nm and a wall thickness of 15 nm. The extremely high length-to-diameter ratio of the L-TNTs was attributed to the viscosity of the organic electrolyte, which could weaken the chemical dissolution of the barrier layers [25]. The TiO_2/ITO film appeared uniform and dense with a thickness of ~160 nm.

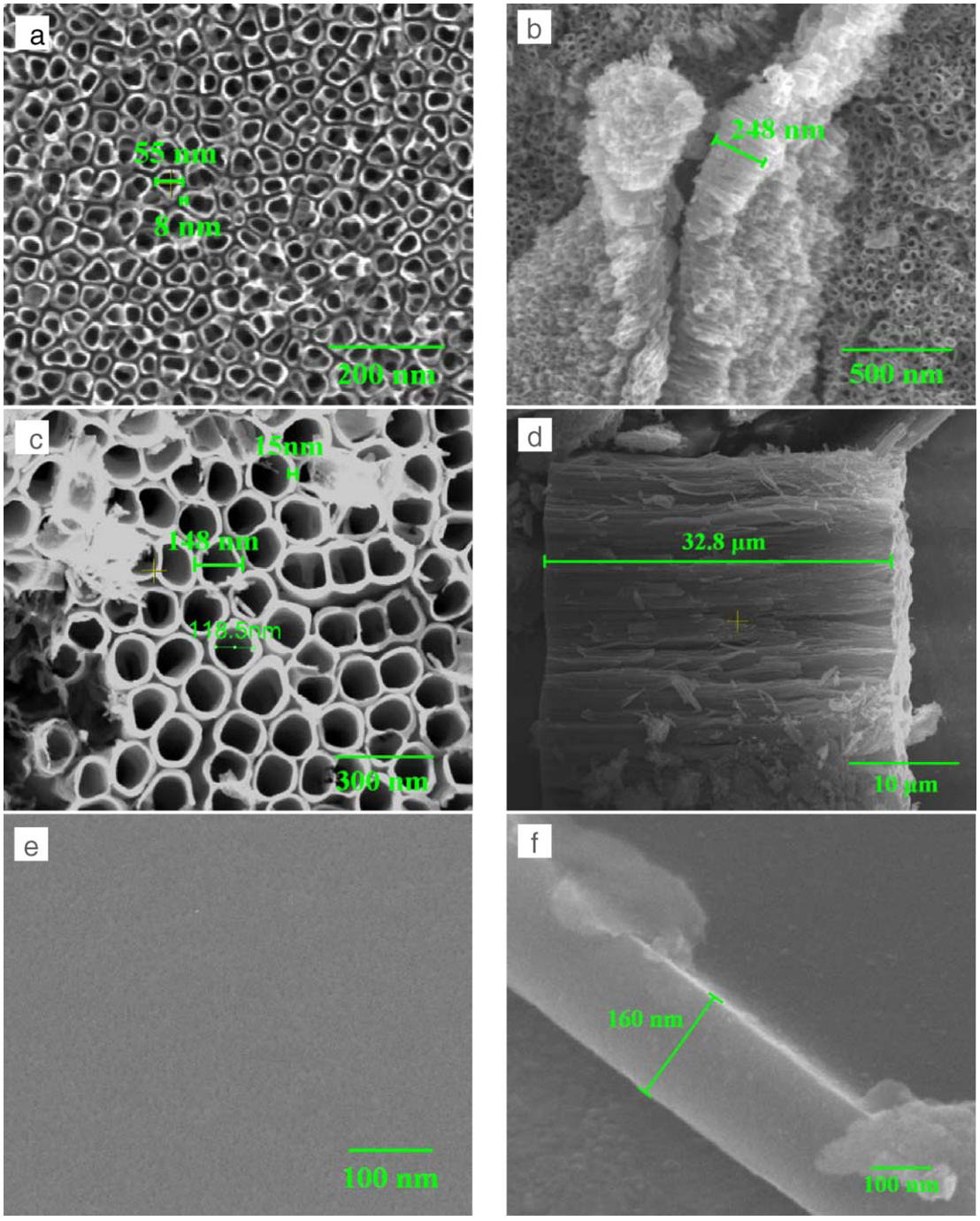

Fig. 1. Top and cross-sectional images of S-TNTs (a and b), L-TNTs (c and d), and TiO_2 thin film (e and f).

The XRD spectra of S-TNTs and L-TNTs are shown in Fig. 2. The prominent peak at 25.3° can be assigned to the (1 0 1) diffraction of anatase TiO_2, indicating the S-TNTs and L-TNTs highly crystalline [26]. The S-TNTs also exhibited many XRD peaks of Ti that did not appear for the L-TNTs. This is because that the L-TNTs were 117 times longer than the S-TNTs, preventing the Ti substrate from being detected by X-rays.

3.2. The PC and PEC reductions of Cr(VI)

3.2.1. The various reductions of Cr(VI) over S-TNTs

Fig. 3(a) compares the reductions of Cr(VI) under a variety of conditions. There was almost no reduction of Cr(VI) observed under the electrocatalytic (EC) condition, suggesting the electrons injected into the photocathode were very few. The conversion ratio of Cr(VI) achieved 27% after 2 h under the photolytic condition, largely ascribed to the photoinduced electron transfer from the citic acid to Cr(VI) [8]. The S-TNTs could present some contribution to the photoinduced reduction of Cr(VI), as the reduction of Cr(VI) under the PC condition was slightly greater than that under the photolytic condition, indicating that there also existed a photoinduced electron transfer from TNTs to Cr(VI). The reduction of Cr(VI) under the PEC condition was the most significant, featuring the virtually complete loss of Cr(VI) after 60 min UV irradiation.

The inset in Fig. 3(a) shows the UV–vis absorption spectra of the reactive solution at various times during the PEC reduction of

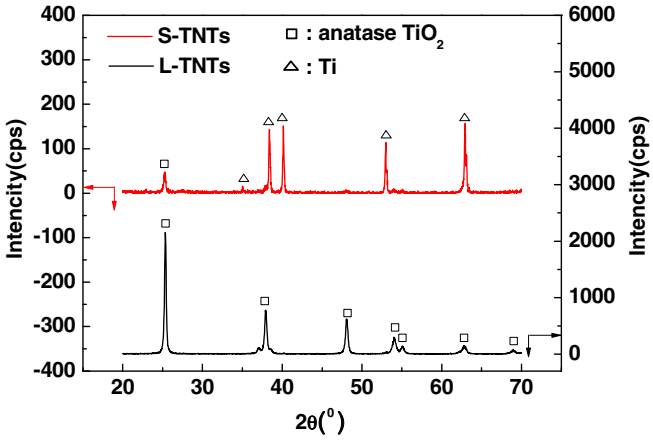

Fig. 2. X-ray diffraction patterns of S-TNTs and L-TNTs.

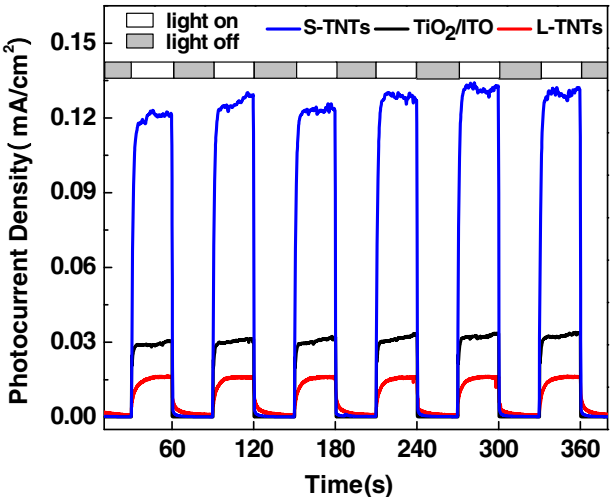

Fig. 4. Transient photocurrent curves of S-TNTs, L-TNTs, and TiO_2/ITO in the 0.5 mM NaCl aqueous solution with a Pt foil as the photocathode.

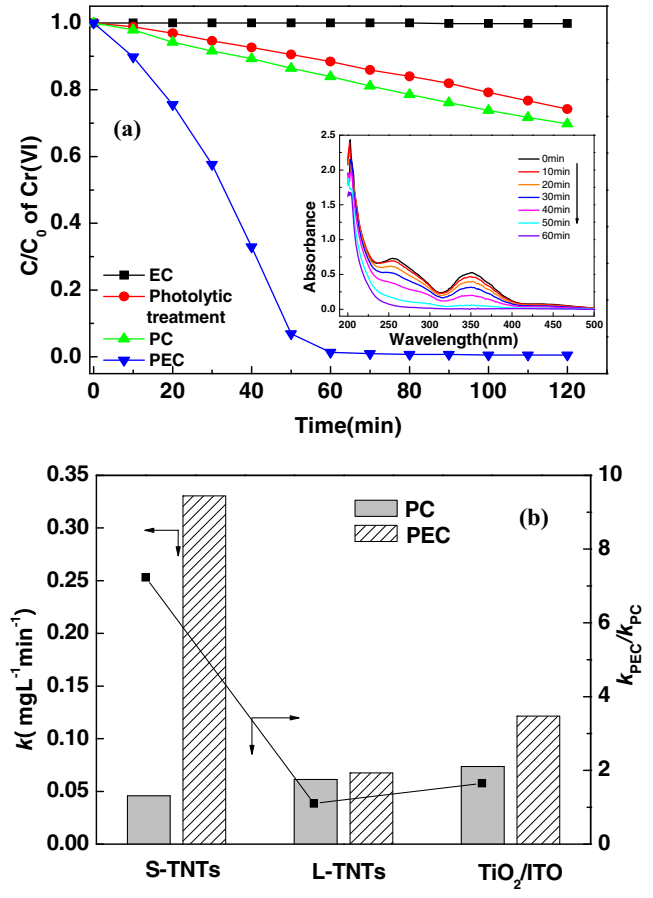

Fig. 3. (a) The photolytic test of Cr(VI) and the EC, PC, and PEC reduction of Cr(VI) over S-TNTs. The reaction condition is initial [Cr(VI)] = 17.7 mg/L, pH = 2.5, initial [citric acid] = 0.5 mM, and [NaCl] = 1 M. For the photolytic test of Cr(IV), there is UV irradiation without S-TNTs and photocathode. For the EC reduction of Cr(IV), there are S-TNTs and photocathode (60 mm × 52 mm Ti mesh) with a bias of 1.5 V and no UV irradiation. For the PC reduction of Cr(IV), there are S-TNTs and photocathode (60 mm × 52 mm Ti mesh) with UV irradiation and no bias. For the PEC reduction of Cr(IV), there are S-TNTs and photocathode (60 mm × 52 mm Ti mesh) with UV irradiation and a bias of 1.5 V. (b) The rate constants of the PC and PEC reductions of Cr(VI) over S-TNTs, L-TNTs and TiO_2/ITO. The EC reduction of Cr(VI) could be neglected as seen in (a). To simplify the evaluation, all the reductions of Cr(VI) were assumed to be zero-order reaction. The inset of (a) is UV–vis absorption spectra of the reaction solution at various times during the PEC reduction of Cr(VI) over S-TNTs.

Cr(VI). It is evident that the two Cr(VI) characteristic peaks at 256 and 349 nm virtually disappeared at 60 min. The residual Cr(VI) concentration at 60 min was measured $\leq$0.2 mg L^{-1}.

The rate constants of Cr(VI) reduction under the PC and PEC conditions were calculated to be 0.046 and 0.33 mg L^{-1} min^{-1}, respectively, suggesting that the bias was able to effectively restrain the recombination of photogenerated excitons in S-TNTs.

3.2.2. Comparison of the three TiO_2 photoanodes

Fig. 3(b) compares the rate constants of the PC and PEC reductions of Cr(VI) over the three TiO_2 photoanodes. The PC rate constants (k_{PC}) were relatively low for all the three anodes, decreasing in the order of TiO_2/ITO > L-TNTs > S-TNTs. The slightly higher k_{PC} of TiO_2/ITO over the TNTs is due to the better transparency of the ITO glass substrate relative to the Ti sheet, leading to the greater exposure of the citric acid to the UV radiation. The L-TNTs possess the better light-trapping capability than the S-TNTs, resulting in more photogenerated electrons and therefore an increased k_{PC} [20].

The PEC rate constants (k_{PEC}) of the three catalysts decreased in the order of S-TNTs $\gg$ TiO_2/ITO > L-TNTs. The ratio of k_{PEC}/k_{PC} was 7.2 for the S-TNTs, compared with that (1.7) for the TiO_2/ITO. This is because the resistance offered by the S-TNTs is lower than that of the TiO_2/ITO [8], resulting in more efficient electron transport and consequently improving the separation of photogenerated excitons. Nevertheless, L-TNTs decelerated the PEC reduction of Cr(VI), due to the following three reasons. Firstly, the electric resistance of nanotube increases as its length, leading to the suppressed exciton dissociation in L-TNTs [20,27]. Secondly, the PEC reduction of Cr(VI) over L-TNTs is hindered due to the splited morphology of the nanotube array [25], as seen in Fig. 1(c). Thirdly, L-TNTs are prone to peel away from the Ti substrate, seting barrier to the electron transfer from L-TNTs to Ti substrate [28].

3.2.3. Photoelectric properties of the three TiO_2 photoanodes

Fig. 4 shows the transient photocurrents in the three TiO_2 anodes under the intermittent UV irradiation. The transient photocurrent density was 0.128, 0.031, and 0.016 mA cm^{-2} for the S-TNTs, TiO_2/ITO, and L-TNTs, respectively. Obviously, the S-TNTs exhibited a much greater photoresponse than L-TNTs and TiO_2/ITO. Indeed, for the three TiO_2 photoanodes, the increasing order of the photocurrent density is coincident with that of the PEC activity, confirming the above analyses about the influences of the TiO_2 structure on the electron conduction.

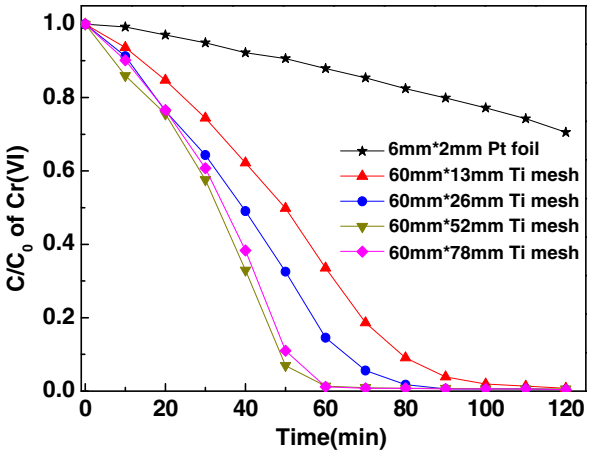

Fig. 5. Effect of the photocathode surface area on the PEC reduction of Cr(VI) over the S-TNTs photoanode. The reactive condition is initial [Cr(VI)] = 17.7 mg/L, a bias = 1.5 V, pH = 2.5, initial [citric acid] = 0.5 mM, and [NaCl] = 1 M.

3.2.4. *Effect of photocathode surface area on the PEC reduction of Cr(VI)*

In the PEC reduction of Cr(VI), the electrons photogenerated in the TiO_2 anode are driven through the external circuit by the applied voltage to the cathode, where the reduction of Cr(IV) takes place. Thus, the surface area of the photocathode might play an important role in determining the rate of Cr(IV) reduction. In quest of the provided issue, the PEC reductions of Cr(VI) using a Pt foil (6 mm × 2 mm) or various-sized Ti meshes as the photocathode were studied. As shown in Fig. 5, the PEC reduction rate of Cr(VI) increased with increasing the surface area of photocathode. The dependence of the PEC reduction of Cr(VI) on the area of the photocathode suggests that the large-area Ti mesh provided plenty of sites where the $Cr_2O_7^{2-}$ ions could be adsorbed and captured by the photogenerated electrons, leading to the efficient reduction of Cr(VI) [3]. It is worth noting the Ti mesh (60 mm × 78 mm) was slightly less efficient than the one (60 mm × 52 mm). This suggests that some factors other than the contact area between $Cr_2O_7^{2-}$ ions and electrons, such as the limited number of photogenerated electrons, the rate of ion exchange at the cathode, accounted for the limitation of the Cr(IV) reduction. The maximum rate of the PEC Cr(VI) reduction was 0.33 mg L^{-1} min^{-1} using S-TNTs as the photoanode and a large-area Ti mesh as the photocathode.

3.3. *Identification of Cr(V) and Cr(III)*

We quantified the amounts of Cr in the three oxidation states, Cr(VI), Cr(V), and Cr(III). Fig. 6(a) shows the EPR spectrum (the inset) and concentration changes of Cr(V) during the PEC reduction of Cr(VI). The signal was centered at g_{iso} = 1.978 with four ^{53}Cr hyperfine satellites; the coupling constant of 18.6 G was in excellent agreement with published reports and attributed to $CrO(CitH_2)_2^-$ [16]. The concentration of Cr(V) was relatively small over the reaction course: it reached a maximum value of approximately 0.0033 mM at 5 min and then decreased steadily to nearly zero at 30 min. This is consistent with the observation reported by Meichtry et al. [29]. The maximun concentration of Cr(V) made up only 0.97% of the initial Cr(VI) concentration, indicating that Cr(V) was an intermediate in the Cr(VI) reduction reaction.

Fig. 6(b) shows the concentrations of Cr(VI) and Cr(III) at various times throughout the reaction. It is evident that the concentration of Cr(VI) decreased steadily, while the concentration of Cr(III) increased accrodingly, with the reaction going on. The concentration sum of Cr(VI) and Cr(III) at a given time remained almost unchanged, again suggesting there was no appreciable accumulation of any intermediate(s). Thus, it is concluded that Cr(III) was the main product in the PEC reduction of Cr(VI), in association with a small amount of Cr(V) as an intermediate.

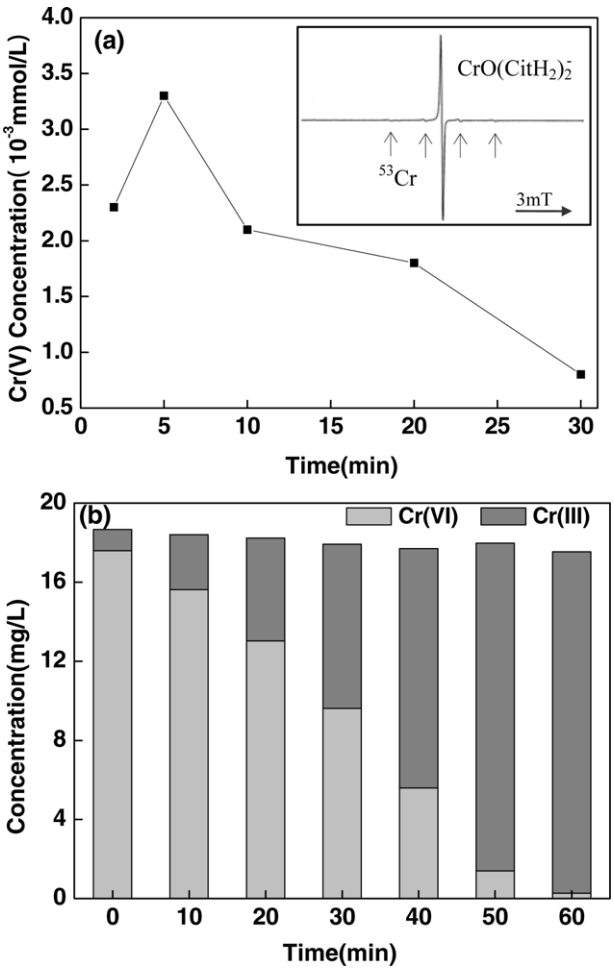

Fig. 6. Concentration variations of Cr(V) (a) and Cr(VI) and Cr(III) (b) in the PEC reduction over S-TNTs. A 60 mm × 52 mm Ti mesh serves as the photocathode. The reactive condition is initial [Cr(VI)] = 17.7 mg/L, a bias = 1.5 V, pH = 2.5, initial [citric acid] = 0.5 mM, and [NaCl] = 1 M. Note that, the initial non-zero concentration of Cr(III) measured at time = 0 may reflects a small systematic error in the method that cannot significantly alter our conclusions. The inset of (a) is the EPR spectrum of the Cr(V)–Cit complex.

3.4. *The mechanism for the PEC reduction of Cr(VI)*

The process of the PEC reduction of Cr(VI) is shown in Scheme 2. Upon the UV irradiation, the S-TNTs are excited, leading to the efficient generation of the hole–electron pairs. Within the S-TNTs photoanode, holes in the valence band (VB) can oxidize adsorbed H_2O into $HO^\bullet$ in the absence of organic compounds, expressed as:

$$h^+ + H_2O \rightarrow HO^\bullet + H^+ \quad (1)$$

When citric acid is present, it is oxidized as follows:

$$h^+ + \text{citricacid} \rightarrow \text{oxidationproduct}, \quad (2)$$

$$HO^\bullet + \text{citricacid} \rightarrow \text{oxidationproduct}. \quad (3)$$

In the meanwhile, the photoelectrons in the conduction (CB) of the photoanode are transferred through the external circuit to the Ti mesh photocathode by the applied voltage, and then captured there by adsorbed $Cr_2O_7^{2-}$, creating the products of Cr(V) and

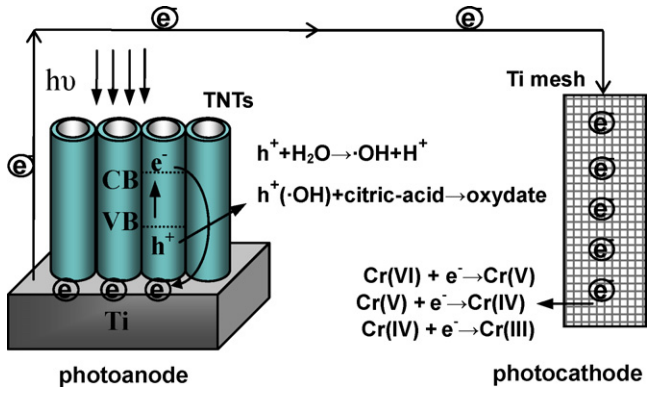

Scheme 2. Schematic illustration of the PEC reduction of Cr(VI) with S-TNTs as the photoanode and a Ti mesh as the photocathode under UV irradiation.

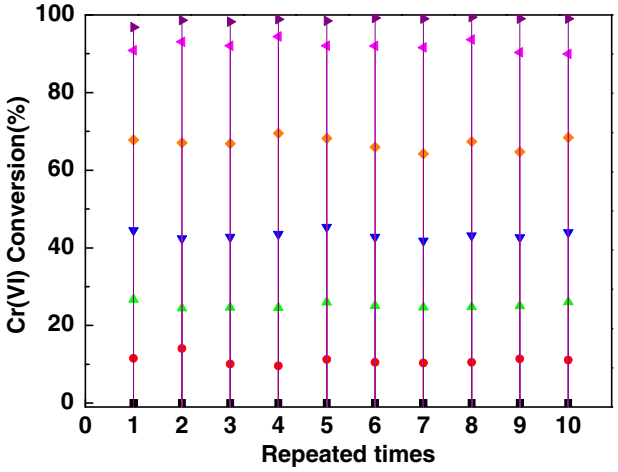

Fig. 7. The repeated PEC reductions of Cr(IV) over S-TNTs. A 60 mm × 52 mm Ti mesh serves as the photocathode. The reactive condition is initial [Cr(VI)] = 17.7 mg/L, a bias = 1.5 V, pH = 2.5, initial [citric acid] = 0.5 mM, and [NaCl] = 1 M.

Cr(III). Though Cr(IV) has not been detected in the experiment, it has been considered as one intermediate as reported [15]. Therefore, it is proposed that Cr(VI) gets reduced via multiple one-electron steps, which can be depicted as follows:

$$\mathrm{Cr(VI)} \xrightarrow{e-} \mathrm{Cr(V)} \xrightarrow{e-} \mathrm{Cr(IV)} \xrightarrow{e-} \mathrm{Cr(III)}. \quad (4)$$

3.5. PEC stability of S-TNTs

In an effort to test the stability of the S-TNTs, the PEC reduction of Cr(VI) was repeatedly carried out using the same S-TNTs photoanode. The result is depicted in Fig. 7. The reduction rate remained almost identical in all 10 trials, indicating the excellent stability of the S-TNTs. Furthermore, it was observed that the S-TNTs could be free from the passivation which was a serious problem for the suspended TiO_2 powder [30]. Therefore, the S-TNTs can be considered as a convenient, stable, and highly efficient catalyst for the PEC reduction of Cr(VI).

4. Conclusions

The PEC reduction of Cr(VI) was optimized using the S-TNTs as the photoanode and a large-area Ti mesh as the photocathode: the nearly complete reduction of 17.7 mg/L Cr(VI) was achieved after 60 min UV irradiation. The conversion process of Cr(VI) into Cr(III) was also quantitatively characterized. The S-TNTs in association with a large-area photocathode, have been demonstrated to be a simple, efficient way to remove liquid-phase Cr(VI).

Acknowledgements

The authors are grateful to the financial support by the National Natural Science Foundation of China (20407002), The National Basic Research Program of China (2002CB410802) and the Special Funds for State Key Joint Laboratory of Environmental Simulation and Pollution Control.

References

[1] M. Costa, Toxicol. Appl. Pharmacol. 188 (2003) 1–5.
[2] Y. Ku, I.L. Jung, Water Res. 35 (2001) 135–142.
[3] S.G. Schrank, H.J. Jose, R. Moreira, J. Photochem. Photobiol. A-Chem. 147 (2002) 71–76.
[4] A. Fujishima, K. Honda, Nature 238 (1972) 37–38.
[5] I.K. Konstantinou, T.A. Albanis, Appl. Catal. B-Environ. 49 (2004) 1–14.
[6] G. Cappelletti, C.L. Bianchi, S. Ardizzone, Appl. Catal. B-Environ. 78 (2008) 193–201.
[7] T. Iwata, M. Ishikawa, R. Ichino, M. Okido, Surf. Coat. Technol. 169 (2003) 703–706.
[8] L.X. Yang, Y. Xiao, S.H. Liu, Y. Li, Q.Y. Cai, S.L. Luo, G.M. Zeng, Appl. Catal. B-Environ. 94 (2010) 142–149.
[9] P. Mohapatra, S.K. Samantaray, K. Parida, J. Photochem. Photobiol. A-Chem. 170 (2005) 189–194.
[10] H. Kyung, J. Lee, W.Y. Choi, Environ. Sci. Technol. 39 (2005) 2376–2382.
[11] T. Papadam, N.P. Xekoukoulotakis, I. Poulios, D. Mantzavinos, J. Photochem. Photobiol. A-Chem. 186 (2007) 308–315.
[12] H. Yu, S. Chen, X. Quan, H. Zhao, Y. Zhang, Environ. Sci. Technol. 42 (2008) 3791–3796.
[13] J. Yoon, E. Shim, S. Bae, H. Joo, J. Hazard. Mater. 161 (2009) 1069–1074.
[14] J.J. Testa, M.A. Grela, M.I. Litter, Langmuir 17 (2001) 3515–3517.
[15] J.J. Testa, M.A. Grela, M.I. Litter, Environ. Sci. Technol. 38 (2004) 1589–1594.
[16] J.M. Meichtry, M. Brusa, G. Mailhot, M.A. Grela, M.I. Litter, Appl. Catal. B-Environ. 71 (2007) 101–107.
[17] L.C. Macedo, D.A.M. Zaia, G.J. Moore, H. de Santana, J. Photochem. Photobiol. A-Chem. 185 (2007) 86–93.
[18] W.H. Leng, Z. Zhang, J.Q. Zhang, C.N. Cao, J. Phys. Chem. B 109 (2005) 15008–15023.
[19] F.M.M. Paschoal, M.A. Anderson, M.V.B. Zanoni, J. Hazard. Mater. 166 (2009) 531–537.
[20] Z. Liu, X. Zhang, S. Nishimoto, M. Jin, D.A. Tryk, T. Murakami, A. Fujishima, J. Phys. Chem. C 112 (2008) 253–259.
[21] D. Gong, C.A. Grimes, O.K. Varghese, W.C. Hu, R.S. Singh, Z. Chen, E.C. Dickey, J. Mater. Res. 16 (2001) 3331–3334.
[22] K. Shankar, G.K. Mor, H.E. Prakasam, S. Yoriya, M. Paulose, O.K. Varghese, C.A. Grimes, Nanotechnology 18 (2007) 065707.
[23] J. Shang, F. Zhao, T. Zhu, Q. Wang, H. Song, Y. Zhang, Appl. Catal. B-Environ. 96 (2010) 185–189.
[24] H. Xu, Y. Wang, J. Anal. Lab. (Chin.) 27 (2008) 34–37.
[25] M. Paulose, K. Shankar, S. Yoriya, H.E. Prakasam, O.K. Varghese, G.K. Mor, T.A. Latempa, A. Fitzgerald, C.A. Grimes, J. Phys. Chem. B 110 (2006) 16179–16184.
[26] J. Zhang, I.W. Boyd, B.J. O'Sullivan, P.K. Hurley, P.V. Kelly, J.P. Sateur, J. Non-Cryst. Solids 303 (2002) 134–138.
[27] Y.B. Liu, B.X. Zhou, J.H. Li, X.J. Gan, J. Bai, W.M. Cai, Appl. Catal. B-Environ. 92 (2009) 326–332.
[28] S. Yoriya, M. Paulose, O.K. Varghese, G.K. Mor, C.A. Grimes, J. Phys. Chem. C 111 (2007) 13770–13776.
[29] J.M. Meichtry, V. Rivera, Y. Di Iorio, H.B. Rodriguez, E.S. Roman, M.A. Grela, M.I. Litter, Photochem. Photobiol. Sci. 8 (2009) 604–612.
[30] N. Wang, Y.Z. Xu, L.H. Zhu, X.T. Shen, H.Q. Tang, J. Photochem. Photobiol. A-Chem. 201 (2009) 121–127.